Novel test method for measuring defects in barrier coatings

DUSTIN BURTON, DON VENTRESCA, AND GREGORY W. WELSCH

ABSTRACT: In the last several years, activity to develop water-based barrier coatings (WBBCs) that meet challenging packaging performance requirements has increased dramatically. Cellulose-based packaging solutions can provide a more sustainable packaging option for replacing single-use plastic-based options like extrusion-based and laminated materials. An advantage of WBBCs is the opportunity to reduce the coating thickness applied, as long as the barrier requirements can be met. A challenge that must be overcome is the ability to maintain a defect and pinhole-free coating layer after coating and drying to retain the barrier performance. Many formulation and coating parameters can affect the barrier coating layer quality; however, methods for detecting more subtle differences in these types of studies are not widely available.

Work was carried out to develop a quantitative technique for detecting and measuring the quantity and size of defects in the barrier coating layer. A test method has been developed using a combination of dyed oil and image analysis to be able to characterize the imperfections in the coating surface. The use of dyed oil serves two purposes. First, it better simulates the types of materials, in this case, oils and grease, for which the barrier coating is expected to hold out. Second, it also provides contrast between the coating and failure points for testing.

An image analysis technique is employed to characterize the number and size of the imperfections. For the former, it reduces the testing time required if a quality control or laboratory technician counts the dots. For the latter, it assists with judgment on the source of the root cause of the imperfection, such as base sheet defects, coating dispersion issues, or perhaps micro-blisters in the coating, as some examples.

To show the benefit of this technique, several pilot coating studies were designed to see if the new technique could be utilized to detect differences in WBBC performance. Both process and chemical variables were evaluated. With refinement, it is believed this technique can be utilized in development work, as well as for a potential quality control technique for manufacturing of coated paper and paperboard products

Application: With the refutation of many current oil and grease resistance (OGR) test methods, it was time to develop a more accurate and easily administered test. The test technique described here is easier to administer, provides the user with better data, and allows the user to better see and identify defects in coated paper that has been exposed to oil and grease.

In the last several years, activity to develop water-based barrier coatings that meet challenging packaging performance requirements has dramatically increased [1]. Cellulose-based packaging solutions can provide a more sustainable packaging option for replacing single-use plastic-based options like extrusion-based and laminated materials. An advantage of water-based barrier coatings (WBBCs) is the opportunity to reduce the coating thickness applied, as long as the barrier requirements can be met. A challenge that must be overcome is the ability to maintain a defect and pinhole-free coating layer after coating and drying to retain the barrier performance. Even a high-quality barrier material will perform poorly if defects exist in the coating layer. Many formulation and coating parameters can affect the barrier coating layer's quality; however, methods for detecting more subtle differences in these types of studies are not widely available.

A test that not only identifies defects in the film, but also measures count, size, and the shape of defects is crucial to further develop WBBC coatings. Although dyed oil applications may have been used by producers in the past, taking this data one step further and making a detailed examination of barrier failures can tell us so much more than a simple qualitative analysis. Using a readily available software product, one can analyze these dots to show that even minor changes in the paper coating process can have an overall change in defect creation, and the frequency, shape, and size of defects created.

Another activity of interest was to determine if we could find a correlation between the size and number of imperfections and their relation to barrier failures. To show the benefit of this technique, several pilot coating studies were designed to see if we could utilize the new technique to detect differences in WBBC performance. Both process and chemical variables were evaluated. With refinement, it is believed this technique can be utilized in development work, as well as for a potential quality control technique for manufacturing of coated paper and paperboard products.

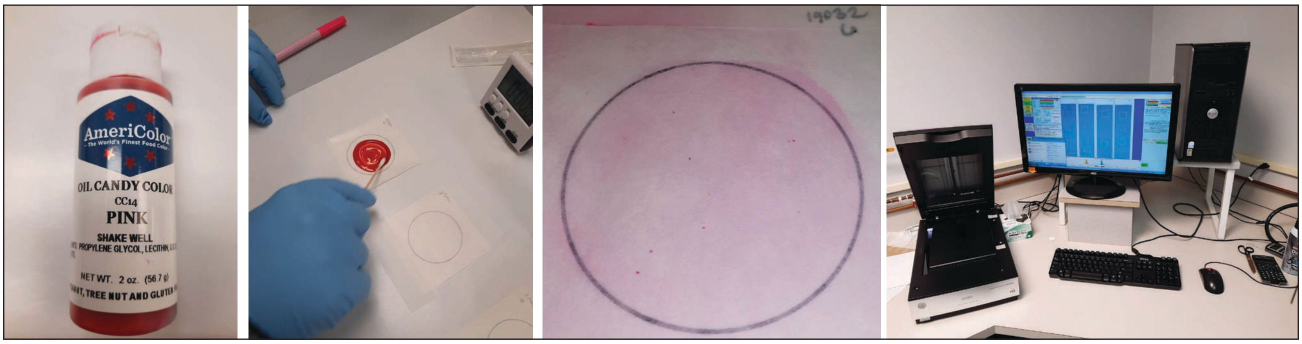

1. Dyed oil, application technique, treated sample after dye application, and test equipment.

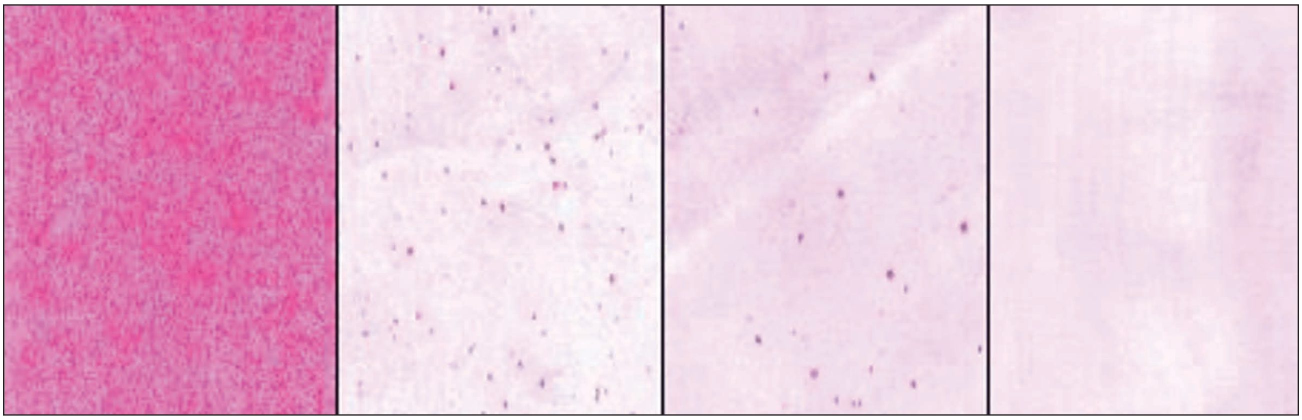

2. Visual representation (after dying) of pinhole improvement with increased coat weight.

BACKGROUND

For years, the 3M Kit test (TAPPI Standard Test Method T 559 "Grease resistance test for paper and paperboard") has been used to test the oil and grease resistance (OGR) performance of uncoated substrates. In those cases, fluorocarbon-based chemicals were used to treat the fiber or used in starch sizing to promote oil and grease resistance. Over time, the method continued to be utilized as a de facto standard for WBBCs applied to paper and paperboard. The industry has reported that, for such WBBCs, Kit test ratings did not always correlate well with package performance in the field, where the barrier is exposed to a variety of oils and/or grease.

If the coated substrate has defects or pinholes, a premature failure may arise. For example, a known WBBC that has passed numerous 3M Kit tests with a value of 12 may give results with a much lower value if pinholes or other defects are present, especially if the defects are not apparent to the human eye. The 3M Kit test fluid drops may simply "settle" into the defect, giving the appearance of a failure. The 3M Kit test is used to test the holdout of the barrier coating or the degree of repellency and/or the anti-wicking characteristics of the coating, not to test if the coated substrate is defect free. So, for the 3M Kit test to give accurate holdout readings, the substrate must first be determined to be defect free. Some procedures require technicians to test around defects, whereas some others may not.

After years of hearing from customers, co-suppliers, and other industry participants that an improvement to the 3M Kit test was needed, we decided to investigate new methods for detecting defects, which are typically the root cause of barrier failures. After a variety of initial experiments, it was discovered that applying dyed oil to the surface of coated substrates helped to identify defects in the coating. After analyzing the samples, it was determined that we could learn more about the defects than simply to read around them; thus, the Defect Characterization test was created.

EXPERIMENTAL

Defect Characterization test – A novel test method for barrier coating quality

A test method has been developed using a combination of a dyed oil and an image analysis technique to be able to count the imperfections quickly and easily in the coating surface. The use of dyed oil serves two purposes. First, it better simulates the types of materials, in this case, oils and grease, for which the barrier coating is expected to hold out. Second, it provides contrast between the coating and failure points for the image analysis after testing. An image analysis technique is then used to characterize the number and size of the imperfections. The technique can reduce the testing time required if a quality control or laboratory technician needs to count the defects. It can also be used to assist with judgment as to the source of the root cause

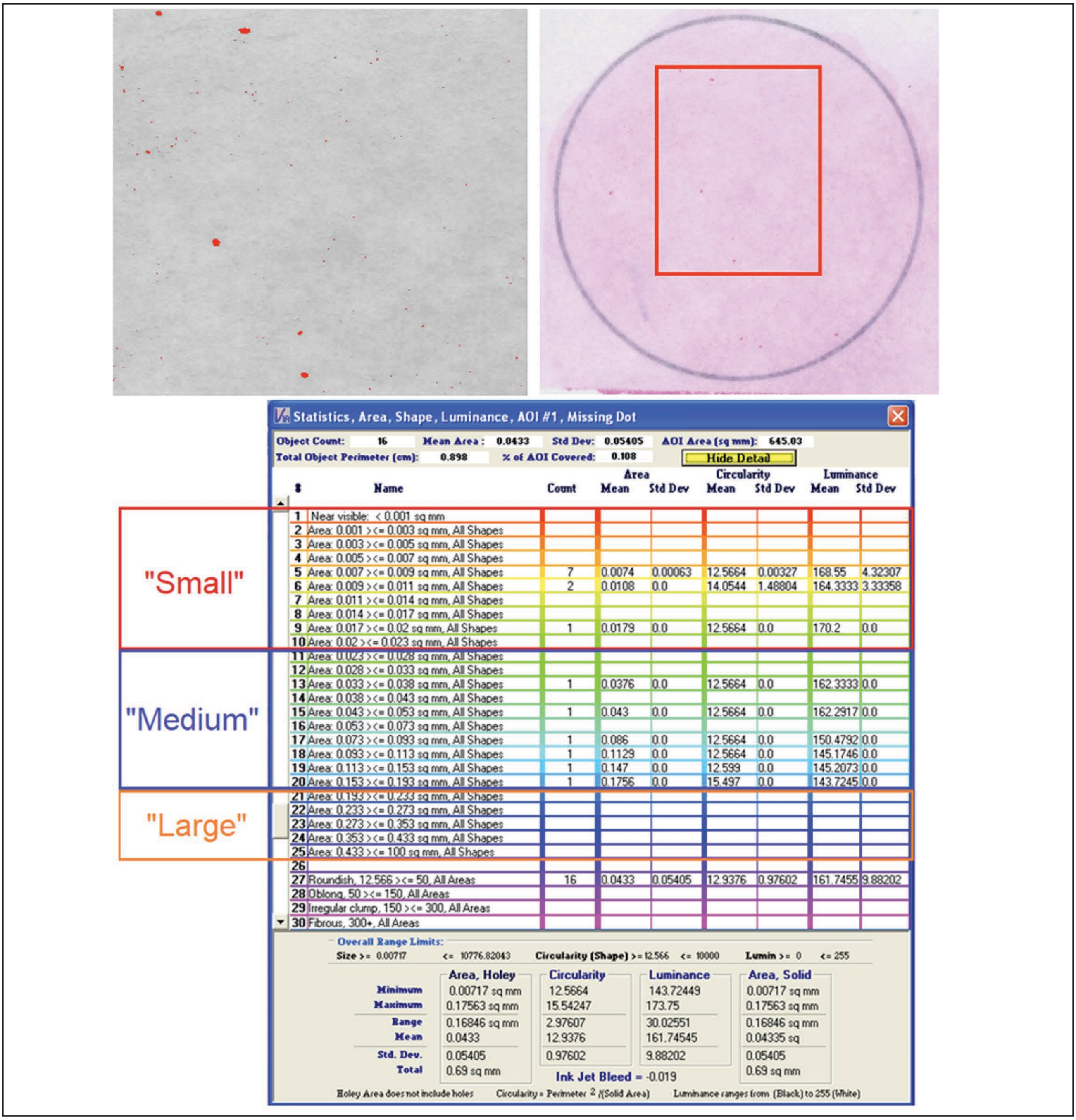

3. Selecting analysis area, exploded image, data, and interpretation.

of the imperfection, such as base sheet defects, coating dispersion issues, or perhaps micro-blisters in the coating, as some examples. Locating these defects can complement other methods used to investigate sources of issues, such as scanning electron microscopy (SEM) techniques.

The Defect Characterization test is conducted by applying a 1-mL quantity of dyed oil to each sample, swirling the dyed oil in a circular pattern covering a 2-in. (5-cm) diameter circle. After the 10 s has expired, the dyed oil that did not penetrate the surface of the sample is removed with an absorbent wipe. The dyed oil chosen for this test is an oil that is typically used in the candy coloring industry. The base ingredient is propylene glycol. The color pink was chosen because it gave the best contrast between defect and white coatings; green- and blue-dyed oils were also evaluated and could also work. We believe other oils could be used, especially if the fluid could be dyed similarly to create the contrast required for good imaging (**Fig. 1**).

After removing the excess dyed oil from the substrate, an image analysis procedure is immediately carried out. The larger defects are readily apparent (**Fig. 2**), but to gain insightful knowledge, such as an accurate count and differ-

Test Element	3M Kit Test	Defect Characterization Test
Area selection	Varies by company; some avoid defects	Any selected area
What is tested?	Spot/drop	Larger sample size
Test area size	~ 0.25 cm^2	6.5 cm^2
Number of fluids applied	1 to 12	1
Fluid selection	See Table VII	Food-grade dyed oil
Estimated test time/sample	5 min	5 min
Equipment cost	Medium*	High**

* Flammable solvents (heptane, toluene) and castor oil mixtures, consumables, fume hood.
** Food-grade oil, consumables, scanner, and image analysis software.

I. Test comparison.

ences in size and shape, we use a combination of an Epson Perfection V750 Pro Scanner (Epson; Suwa, Nagano, Japan) and Verity IA software (Verity IA Software; Milwaukee, WI, USA).

The program and scanner were originally set up for measuring mottle on printed samples by extracting certain color variations. An additional feature in the software included dot count. By using the dyed oil, the defect-free areas remain a light pink color, while the defects absorb more of the dyed oil, giving it a dark pink appearance. By adjusting the sensitivity setting in the image analysis program, we can easily extract the darker-colored dots from the lighter-colored background. The program then counts all the imperfections and categorizes them by size, and if desired, shape as well. This data can be quite relevant in the paper coating industry because one can change the frequency and size of imperfections based on trial conditions (formulation changes, base paper changes, dryer condition changes, etc.), as we will attempt to illustrate in our work.

The most relevant results (**Fig. 3**) derived from the Defect Characterization test are the total count of defects and their sizes or cumulative area. The software can detect dots in the scanned image that are nearly invisible to the human eye. For this work, the dots are categorized into three different sized segments: small, medium, and large. Small dots range in size from < 0.001–0.023 mm^2. Medium dots range in size from 0.023–0.193 mm^2. Large dots are anything greater than 0.193 mm^2. When analyzing samples, the area analyzed is a 6.5 cm^2 sized measurement of the applied oil. This is what has been selected, but it could be modified as needed.

When comparing the new Defect Characterization test method to other barrier testing methods, we believe the key advantage is in assisting with troubleshooting the root cause of failures, i.e., defects. As with most coating applications, even if the paper and coating design are optimized to meet the intended barrier application requirements, the coating process must be executed with minimal-to-zero quality issues. Existing test methods do not adequately help with that analysis. In some cases, procedures state to test around obvious defects. Another benefit of the new test method is in eliminating the need for hazardous chemicals and reducing the time to check the coated sheet. A comparison of the Defect Characterization test against the 3M Kit test can be found in **Table I**.

Dot size and count seems to be sufficient data for most applications, but future work may include a further analysis

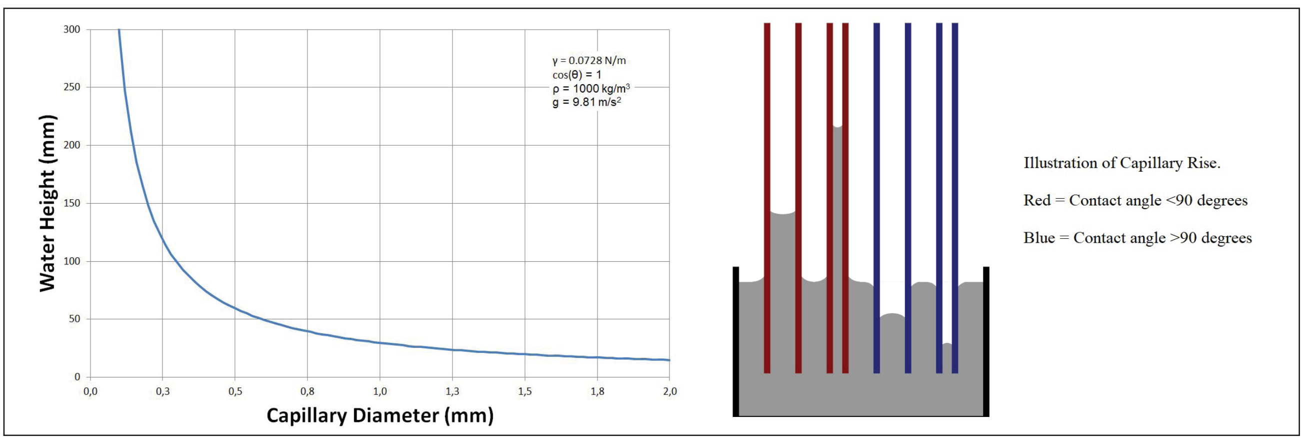

4. Relationship of capillary height vs. capillary diameter (left) [2] and vs. surface tension (right) [3].

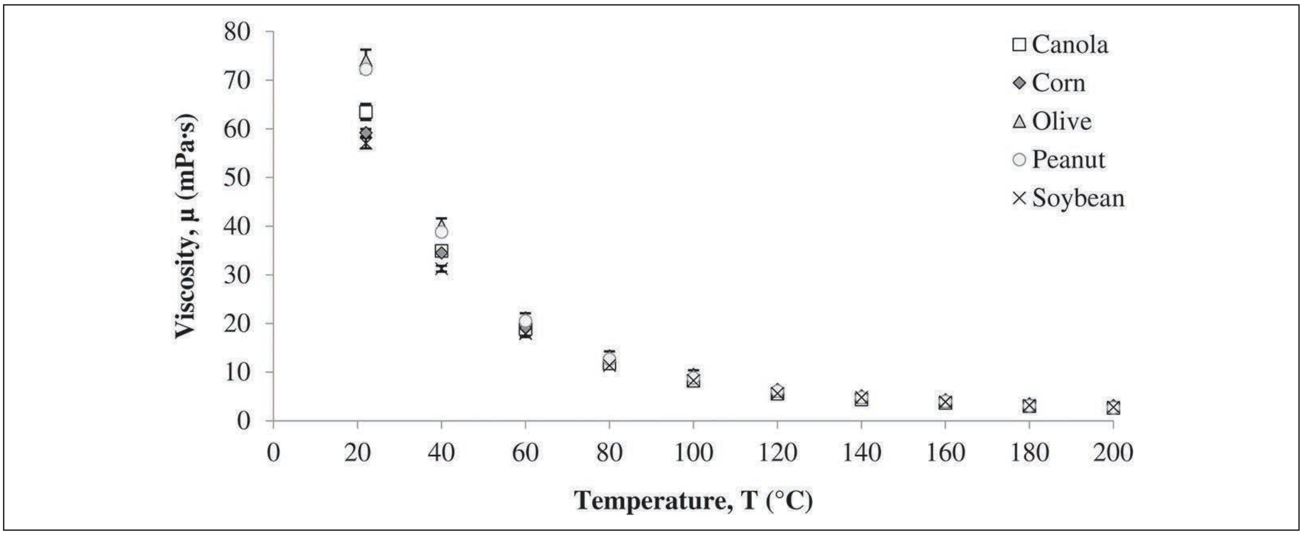

5. Viscosity vs. temperature for five oil types [4].

of data. Data such as dot shape, circularity, blister identification, microscopic evaluation of dyed substrates, and cross-sectional imaging of dyed substrates may be evaluated.

Correlation of Defect Characterization test and barrier testing

Another activity of interest was to determine if we could find correlations between the size, number, and cumulative area of imperfections and their relation to barrier coating failures when tested with two different OGR testing methods (to be described later).

For this evaluation, we consider the defects in coatings to be porous, similar to a capillary. Many references can be found that discuss the role capillary forces can play in fluid transport, and they typically refer to the Young-Laplace equation where a pressure differential can induce fluid transport in capillaries. When the equation (see Appendix for all equation references) is further simplified for capillary flow, it is shown that differential pressure is proportional to the surface tension of the fluid and is inversely related to the radius of the capillary. Higher capillary pressure can give rise to higher fluid transport in smaller diameter capillaries (**Fig. 4**). This suggests smaller capillaries can transport fluid to a greater extent or height in a column than larger capillaries.

If we assume that the defects or pores are capillaries, then many small- or medium-sized capillaries may be as problematic as the large, more obvious defects from the perspective of oil or grease transport. It is also known that for laminar flow in a pipe or tube, Poiseuille's law states the flow rate is inversely proportional to the fluid viscosity. Therefore, more viscous materials will not travel as far in a capillary as those with a lower viscosity. This is important, as testing with materials that do not represent either the viscosity or surface tension of the fluid in question could lead to erroneous results. This again is one aspect of the 3M Kit test we were trying to address by developing a new technique to focus on defect analysis. Also, from Poiseuille's law, we know that as the length of the tube increases, the flow will decrease as well. This suggests, and is also intuitive, that for higher coat weights (i.e., coating thickness), fluid transport is slower, as the capillaries would be longer. This also suggests that in any place where a defect exists, the capillary is shorter and transport times will be faster for the fluid. Again, all equations discussed here can be found in the Appendix.

In many cases, barrier coatings need to perform when in contact with fluids that change viscosity based on conditions of use. One example is in fast food applications where hot food is introduced against the surface of the container. Initially, the oil or grease is quite hot and has significantly lower viscosity than what is experienced at room temperature after cooling (**Fig. 5**) [4]. In these cases, the viscosity of the fluid at 100°C is 5 times lower than at room temperature. As described earlier, differential pressure is proportional to viscosity, so in this case, the ability for hot oil to transport through a capillary would be 5 times greater than oil that has cooled to room temperature. A similar relationship occurs with surface tension, for which for the same oil types are shown in **Fig. 6** [4]. The relation with surface tension suggests that a fluid with lower surface tension could travel faster through a capillary vs. a fluid with high surface tension.

The purpose of this review is to draw attention to the fact that the selection of one material or test condition may not adequately represent the actual conditions of use. Hence, the strategy to make sure the barrier coating is thoroughly tested for defects may provide the best method for ensuring that a quality coated sheet is produced. If one can produce a defect-free coating and the design of the coating is such that it performs when no defects are present, then a quality barrier product would be produced. Although not

T (°C)	γ_{oil} (mN/m) Canola oil	Corn oil	Olive oil	Peanut oil	Soybean oil
Determined using KRÜSS goniometer					
23 ± 0	$31.3 \pm 0.3^{b,c}$	$31.6 \pm 0.1^{a,b}$	31.9 ± 0.0^{a}	$31.3 \pm 0.1^{b,c}$	$31.3 \pm 0.4^{b,c,d}$
40	$30.5 \pm 0.2^{e,f}$	$30.7 \pm 0.1^{d,e}$	$30.9 \pm 0.0^{c,d,e}$	$30.3 \pm 0.2^{e,f}$	30.6 ± 0.3^{e}
60	29.6 ± 0.2^{g}	29.7 ± 0.1^{g}	$30.0 \pm 0.0^{f,g}$	29.7 ± 0.0^{g}	$29.9 \pm 0.0^{f,g}$
80	28.6 ± 0.2^{h}	$28.5 \pm 0.1^{h,i}$	28.8 ± 0.2^{h}	28.8 ± 0.1^{h}	28.7 ± 0.4^{h}
100	27.7 ± 0.1^{j}	27.7 ± 0.1^{j}	27.7 ± 0.0^{j}	27.7 ± 0.1^{j}	$27.9 \pm 0.1^{i,j}$
120	26.5 ± 0.1^{k}	$26.4 \pm 0.2^{k,l}$	26.6 ± 0.1^{k}	26.5 ± 0.0^{k}	27.0 ± 0.0^{k}
140	$25.6 \pm 0.2^{m,n}$	25.3 ± 0.2^{n}	$25.7 \pm 0.5^{m,n}$	$25.5 \pm 0.1^{m,n}$	$25.9 \pm 0.1^{l,m}$
160	24.6 ± 0.1^{o}	$24.1 \pm 0.1^{o,p}$	$24.3 \pm 0.0^{o,p}$	24.5 ± 0.0^{o}	24.5 ± 0.3^{o}
180	$23.5 \pm 0.0^{q,r}$	$23.0 \pm 0.3^{r,s}$	23.1 ± 0.1^{r}	$23.0 \pm 0.1^{r,s}$	$23.8 \pm 0.1^{p,q}$
200	22.4 ± 0.1^{t}	22.0 ± 0.2^{t}	–	21.3 ± 0.4^{u}	$22.5 \pm 0.1^{s,t}$

6. Comparison of surface tension values for five oils at different temperatures [4].

evaluated here, the authors believe the new Defect Characterization test method could be modified to utilize other dyed oils to better simulate the application of interest.

Pilot coater conditions

A series of pilot coater trials (**Table II**) were run at the Trinseo LLC pilot coater located in Midland, MI, USA (**Fig. 7**) to evaluate both process and chemical variables on pinhole/defect formation and corresponding relationship to OGR performance. Barrier coating systems were coated on a flooded nip coater at 1500 ft/min (450 m/min) with a rigid blade using a coat weight ladder approach typically ranging between 5.5 to 11.5 g/m² (3 to 7 lb/3300 ft²). For each coat weight, drying was adjusted in a balanced, stepwise fashion across the air flotation dryers to target 4.3% moisture at the reel. The one exception to this was in Study II, where a coat weight of 6.7 g/m² (4.0 lb/3300 ft²) was targeted and drying was changed as described later. All barrier coated paper was back side-coated to prevent curl with a conventional pigmented paper coating targeting 6.7 g/m² (4 lb/3300 ft²). A coat weight ladder approach was utilized for two reasons. First, this allowed the data to be statistically modelled for drawing firmer conclusions on the new test method. Second, we know fiber coverage is a critical aspect in delivering appropriate barrier performance, so it was important to ensure we had a range in coat weight that would, in the end, produce conditions that were satisfactory in performance to draw sound conclusions. In each case, a single layer of a styrene-acrylate-based starch-containing emulsion system was utilized. In some cases, variations of this system are also described, if applicable in each study.

Study	Pilot Coater Objective Description
I	Base sheet comparison
II	Drying strategy and coalescing aid
III	Barrier system type

II. Pilot coater study description.

Study I – Base sheet comparison

Papermakers have a multitude of variables to consider when it comes to the design of their paper. Improvements are, however, often limited by process constraints or cost drivers in materials. At the same time, they must consider how to balance the design of the base sheet for a barrier grade against the needs for the majority of their production. There are also cost considerations related to transitions to steady-state when moving from grade to grade. Since base sheet design is extremely important for nearly all coated paper performance requirements, the first step was to evaluate how sensitive the new test method could be in detecting a standard from a higher-performing base sheet.

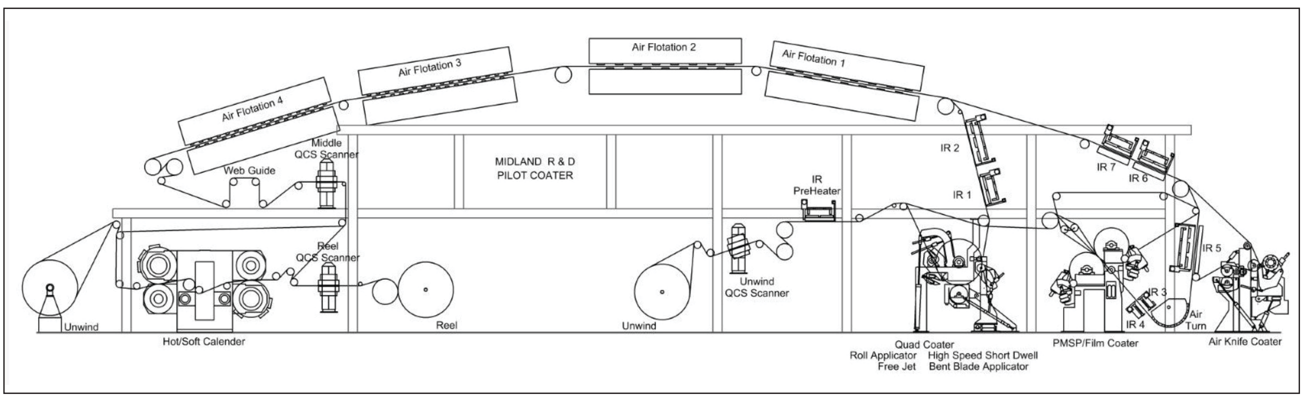

7. Trinseo pilot coater (Midland, MI, USA) layout and dryer configuration.

Base Sheet	Basis Weight — Uncoated	Roughness, um	Porosity, s
H	64 g/m^2 (38 lb/3300 ft^2)	5.2	55
I	80 g/m^2 (48 lb/3300 ft^2)	4.7	154

III. Base sheet description Study I.

Drying Strategy	Drying Strategy Description	Final Moisture
Balanced	Moderate temperatures and nozzle velocities across the 4 AF dryers	4.5%
Early AF	Higher temperatures and nozzle velocities in first 2 of the 4 AF dryers	4.5%
Late AF	Higher temperatures and nozzle velocities in last 2 of the 4 AF dryers	4.5%
IR, Early AF	IR1 used with Early AF strategy	4.5%
IR, Late AF	IR1 used with Late AF strategy	4.5%
IR, Early AF	IR1 used with Early AF strategy	2.0%
IR, Late AF	IR1 used with Late AF strategy	2.0%
AF = forced air flotation; IR1 = 2 rows of gas-fired infrared (IR) drying.		

IV. Drying strategy descriptions Study II.

Two different woodfree base sheets were evaluated to see if the new defect test method was able to detect differences in the two designs. A rougher sheet makes it more challenging to achieve a uniform barrier coating without defects, especially at low coat weights. Rougher sheets can promote more air entrainment during coating as air is trapped between the paper surface and the coating layer during application; during drying these may appear as bubbles or craters if they are trapped during coating coalescence. Sheet porosity also plays a role, as it has a significant effect on coating penetration. In this case, details on furnish type, filler, or other process variables were not provided by the supplier. However, indications were given that Base Sheet I should perform better as a base paper for a single-coated barrier than Base Sheet H. We looked for indications of fewer pinholes at equal coat weight, as well as the potential difference in the distribution of small, medium, and large pinholes. Some basic base sheet tests results are shown in **Table III**.

Study II – Drying strategy and coalescing aid

The influence of the drying strategy has been studied as it relates to end-use performance properties and in water-based barrier coatings on paper [5,6]. Many water-based barrier coatings are typically quite high in binder content and are formulated below the critical pigment volume concentration. To cure these systems, water vapor must transport out of the coating and not contribute to defect formation in the form of micro-blisters or other defects.

In this work, we use the Defect Characterization test method to evaluate if a higher frequency or certain dot size can be detected. Five different drying strategies were evaluated on the pilot coater for a common barrier system and base sheet, as shown in **Table IV**. In the table, AF is used to represent the 4 forced air flotation dryers, and IR1 is used to represent the 2 rows of gas-fired infrared (IR) drying (Fig. 7). Also evaluated were two different final moisture contents for the two IR conditions, including a very low moisture condition to represent harder drying conditions.

Barrier System	Description
B	Proprietary SA-SCE Barrier System
C	Barrier System B with 1.0 parts coalescing aid

V. Barrier system description for Study II.

It is typical in architectural coatings with film-forming binders to use a coalescing aid to soften the polymer by lowering the glass transition temperature to assist in film formation and binder coalescence. In those cases, drying is typically done in ambient conditions with slow water transport. For barrier coatings containing high levels of binder, some have suggested that coalescing aids could improve film formation and reduce defects. In this evaluation, we decided to evaluate the use of a coalescing aid, glycerol, as a system component (**Table V**). For Barrier System C, glycerol was added at a level of 1 part to Barrier System B. This was assessed within the same drying evaluation described previously.

Barrier System	Description	Coating Surface Tension, dynes/cm	Paper Total Surface Energy, mN/m
X	Proprietary SA-SCE Barrier System X	46.5	58
Y	Barrier System X with 0.5 parts higher surfactant	37.4	52
Z	Proprietary SA-SCE Barrier System Z	N/A	54

VI. Barrier system description for Study III.

Rating	Castor Oil, g	Toluene, ml	Heptane, ml
1	969	0	0
2	872	50	50
3	775	100	100
4	678	150	150
5	581	200	200
6	485	250	250
7	388	300	300
8	291	350	350
9	194	400	400
10	97	450	450
11	0	500	500
12	0	550	550

VII. Kit test solutions.

Study III – Barrier system comparison

It has been well documented that the wettability of a substrate can play an important role in the ability of the coating to wet out and stretch to cover the substrate to prevent craters and coating defects [7]. To test that theory, Barrier System Y was evaluated by adding 0.5 parts of a common wetting agent (sodium dioctyl sulfosuccinate) to Barrier System X. Coating surface tension values and their impact on the coated paper surface energy are shown in **Table VI**, as well as the impact on the coated paper surface energy. A third condition was also evaluated, as shown in Table VI, with another proprietary change made to the same SA-SCE barrier system, shown as Barrier System Z. The purpose of this study was to demonstrate whether the new test method was capable of detecting differences between materials and process changes.

Comparative barrier test methods

3M Kit test

The 3M Kit test measures the repellency or anti-wicking behavior of paper and paperboard when subjected to various oils/solvents and was conducted per the TAPPI Standard T

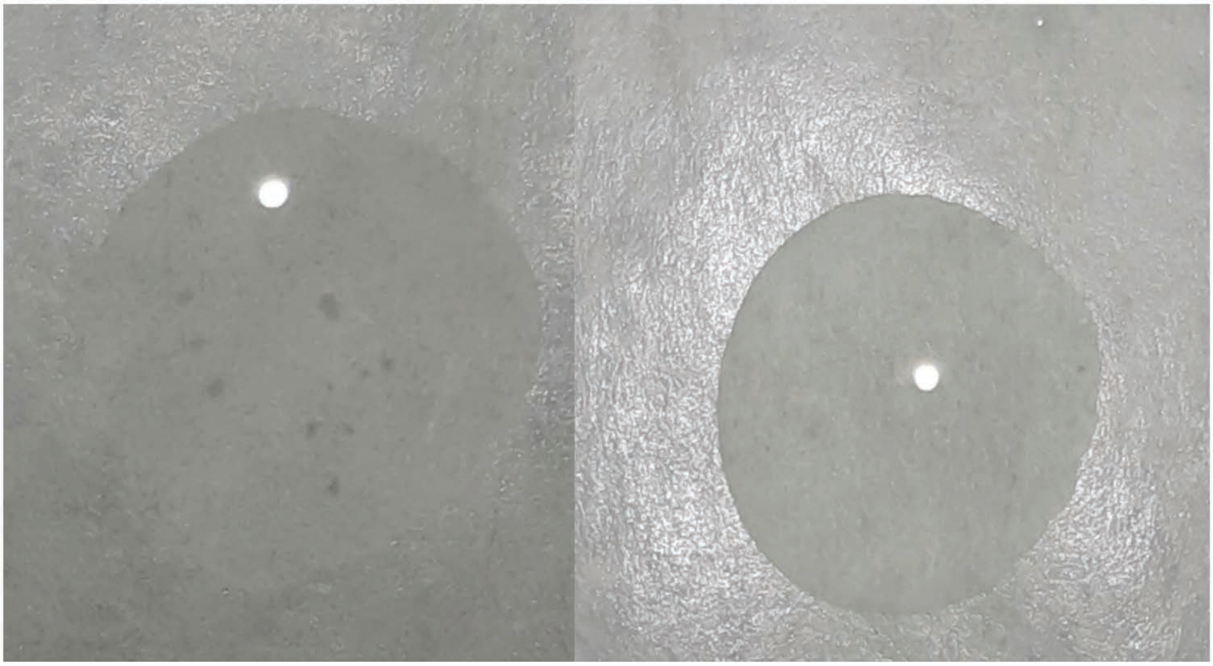

8. Example of a "failed" sample (left) vs. a "passing" sample (right).

Rating	Characterization	Description
0	No penetration	No visible pinholes, spots, or stains.
1	< 10 pinholes	More than 1 pinhole, less than 10 pinholes visible.
2	< 25 pinholes	More than 11 pinholes, less than 25 pinholes visible.
3	< 50 pinholes	More than 26 pinholes, less than 50 pinholes visible.
4	> 50 pinholes	More than 50 pinholes visible.
5	Small spots	Small spots visible.
6	Large spots	Large spots visible.
7	Stain(s)	One or more stains, not able to tell if sample is penetrated.
8	Stain/fail	Stain is kept within barrier ring but has penetrated the sample.
9	Complete fail	Stain goes beyond barrier ring or has caused ring to lift.

VIII. Hot Oil Circle test failure rating system descriptions.

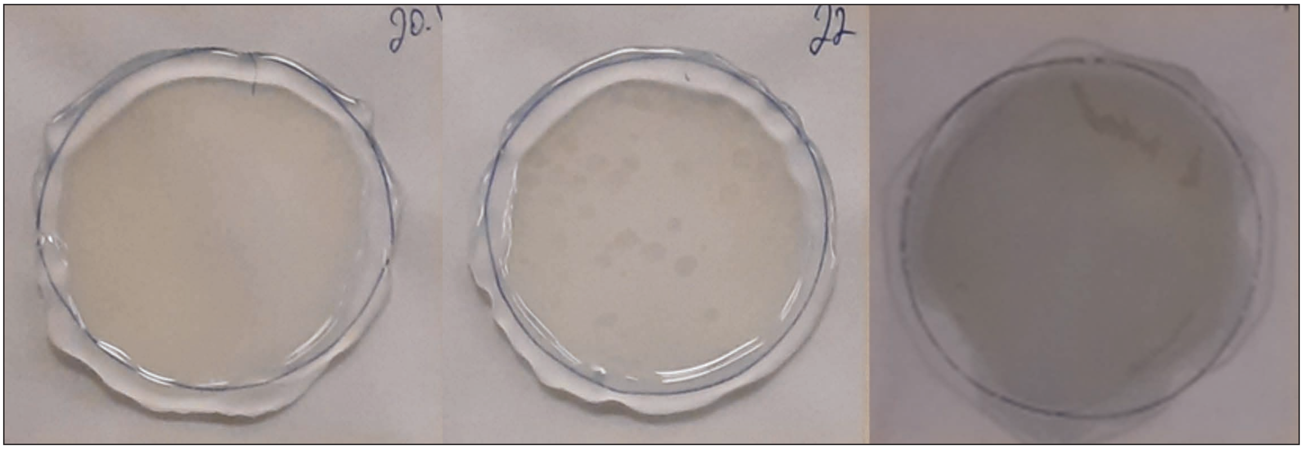

9. Example of a rating of 0 (left; no penetration), a rating of 3 (center; >26 but <50 pinholes), and a rating of 9 (right; complete fail).

559. Kit testing was conducted on flat samples. A series of Kit solutions was prepared using combinations of castor oil, toluene, and heptane, as shown in **Table VII**. A lower Kit value represents a "less harsh" treatment (higher percentages of castor oil), while a high Kit value represents a "harsher" treatment (higher percentages of toluene and heptane).

Higher values, therefore, indicate better barrier performance. The liquid is applied to the substrate using a dropper. A single drop is evaluated for 15 s. After 15 s have expired, the substrate is examined for failures in the coating (typically a stain or pinhole). If considered a failure, a less harsh Kit solution is tested until a sample has passed the examination (drop sits on top of the substrate without penetration or staining). This Kit solution would be recorded as a "pass" for results. **Figure 8** shows testing examples.

Hot Oil Circle test

The Hot Oil Circle test is used to analyze oil barrier properties. Preheated oil (corn oil at 60°C) is applied to the barrier surface. Various time treatments are evaluated from immediate to 24 h. The front (coated) and the back side of the paper samples can be evaluated for oil stain penetration. For this study, testing was carried out at room temperature. Visual observations were made prior to testing and immediately after applying the tempered oil. Observations were also conducted 15 min, 30 min, 45 minutes, 60 min, and 24 h after oil exposure.

Examples may be found in **Figure 9**, and **Table VIII** describes the internally used rating system.

RESULTS AND DISCUSSION

For each of the three pilot coater studies, the new test method was utilized to generate the defect data set for each set of samples. Within the data sets, we looked for any correlations between the types of defects in size, frequency, and area, along with the resulting barrier test results. A summary of the coating run data and formulation tests can be found in the Appendix for the appropriate studies.

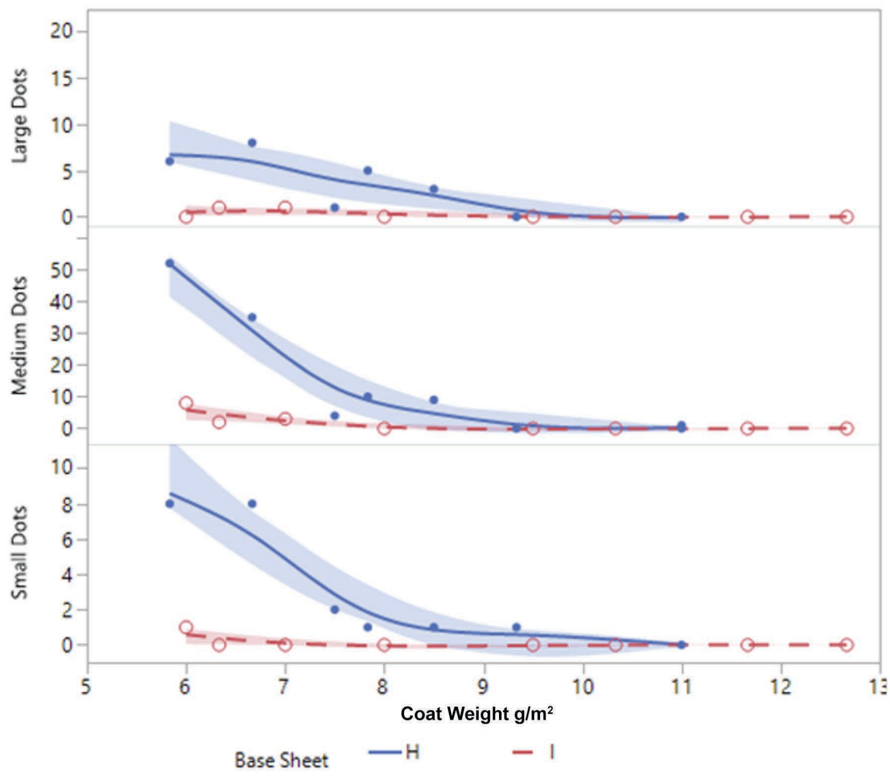

10. Dot size and dot count vs. coat weight for each base paper.

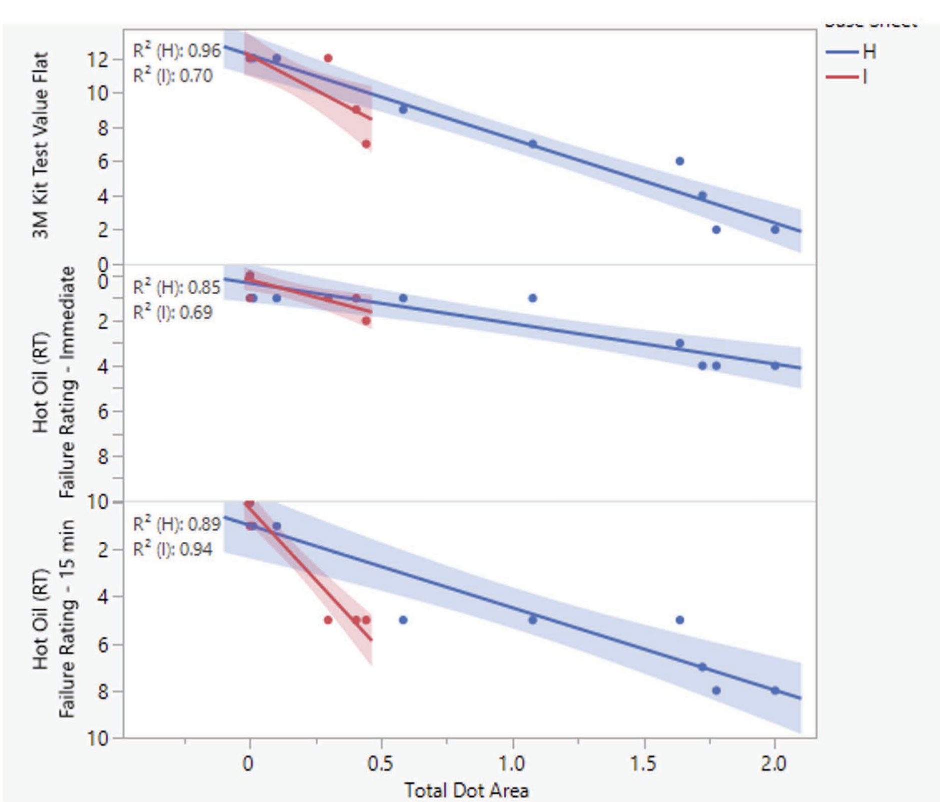

11. Barrier performance vs. total defect area (R^2 = coefficient of determination).

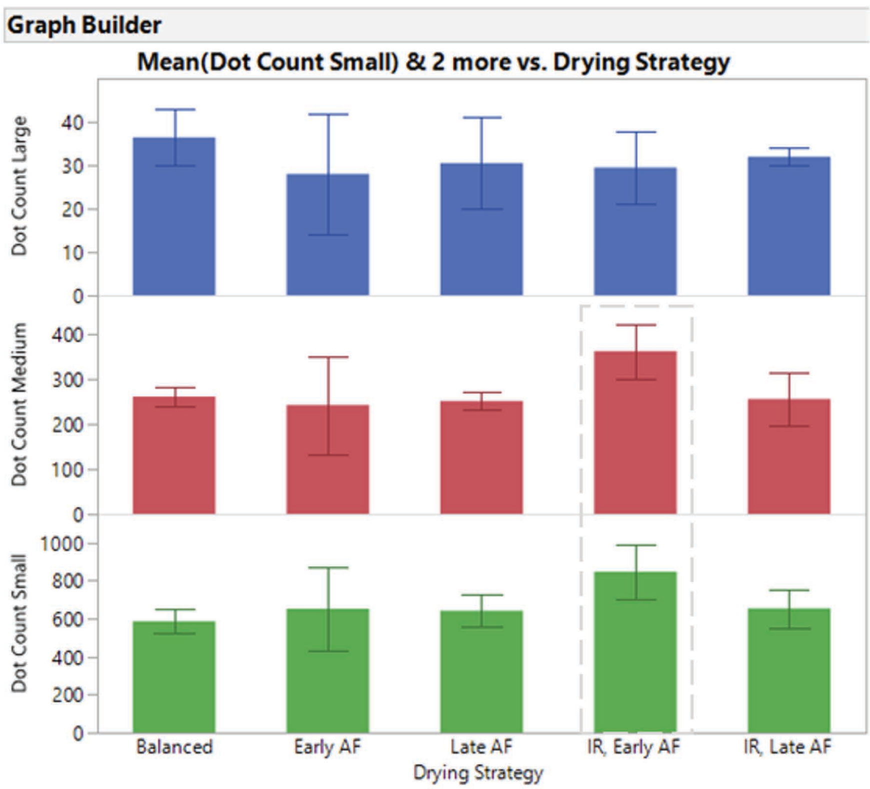

12. Effect of drying strategies in Study II. See Table IV for descriptions of drying strategies.

Study I – Base sheet comparison

For this evaluation, a simple dot plot with a smoothed line fit was constructed comparing, for each dot size (large, medium, small), the dot count vs. applied coat weight for all trial conditions over each base sheet. These results were generated using the Defect Characterization test method. In this case (**Fig. 10**), it was very apparent that Base Sheet I had dramatically fewer dots of all three dot classifications than Base Sheet H. A significant improvement in the small-sized dots ranging from >0.001–0.022 mm2 and the medium-sized dots ranging in size from 0.023–0.193 mm2 was observed.

Data from the Defect Characterization test was evaluated for correlation against two barrier test protocols, the 3M Kit test and a Hot Oil Circle test, both described earlier. For the hot oil test, two time treatments (immediate and 15 min) are compared. For both papers, lower measured defect area (dot size times frequency), as determined from the image analysis of the stained area, correlated well with both test methods (**Fig. 11**).

Study II – Drying strategy and coalescing aid

As described earlier in the Experimental section, Study II was aimed at identifying whether various drying strategies could influence defect formation in WBBC systems. Additional activity was to evaluate the use of a coalescing aid in this type of system to seal off the film through more complete coalescence of the binder materials, as the hypothesis. In this case, a non-optimized base sheet was used, so defect counts are quite high. Defect data was collected utilizing the new test method. **Figure 12** shows the comparative dot counts for all three classifications of dot size and indicates that high energy IR drying combined with harder early air flotation drying promoted the generation of more medium and small defects. Most other drying strategies are comparable and show a lower level of defects.

The comparison considered like conditions where the effect of coalescing aid, described as Barrier System C, was compared to the system without coalescing aid, Barrier System B (**Fig. 13**). In the case of Barrier System C, the effect of the glycerol addition resulted in a statistically significant increase in defects, especially in the medium and small classification. Although glycerol has a very high boiling point (290°C), evaporation can occur above 20°C and in aqueous mixtures. This could explain why the selection of this material and drying at elevated temperature led to more defects, perhaps from microblisters migrating through the coating during consolidation and film coalescence.

For the conditions with an IR drying strategy (many coated paper machines today use some), a lower moisture target (2.7%) was also evaluated. **Figure 14** shows the re-

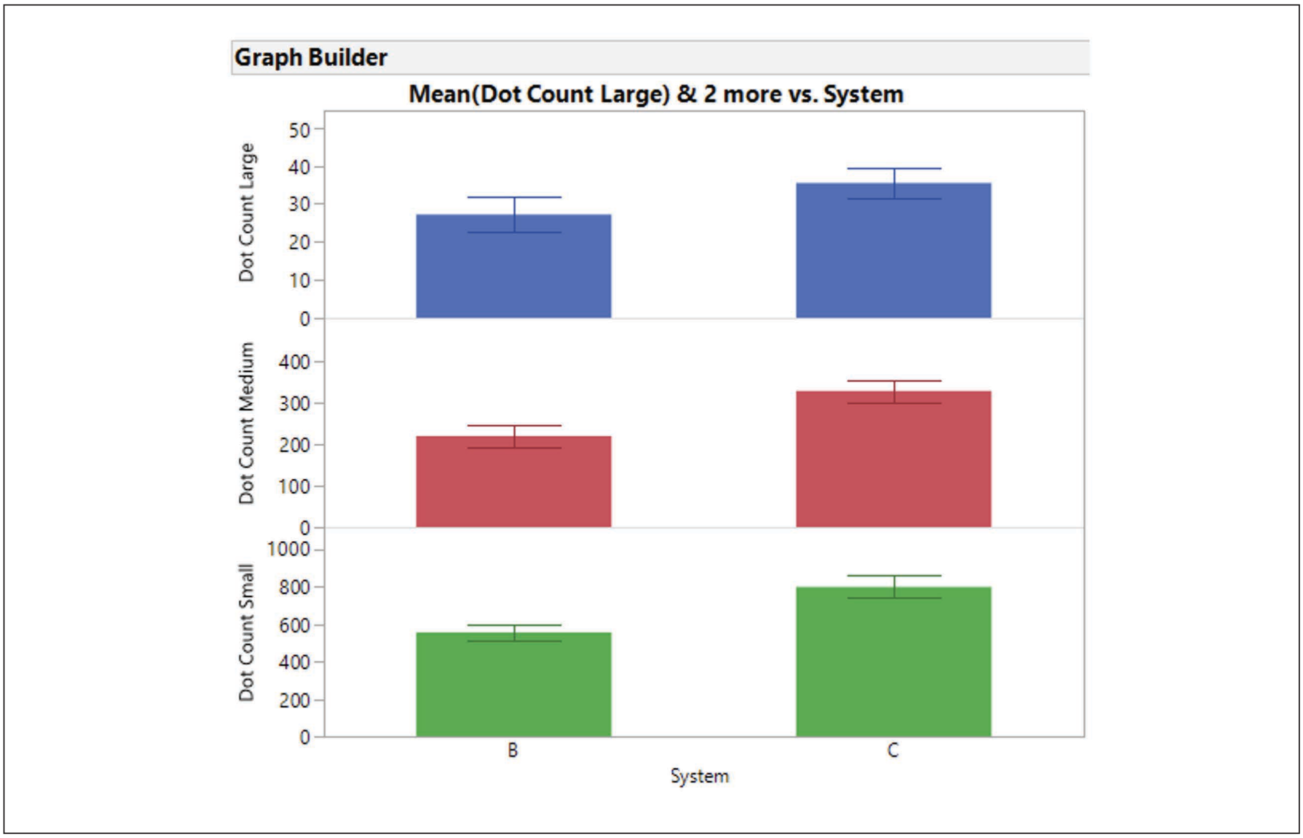

13. Effect of coalescing aid (B = no, C = yes).

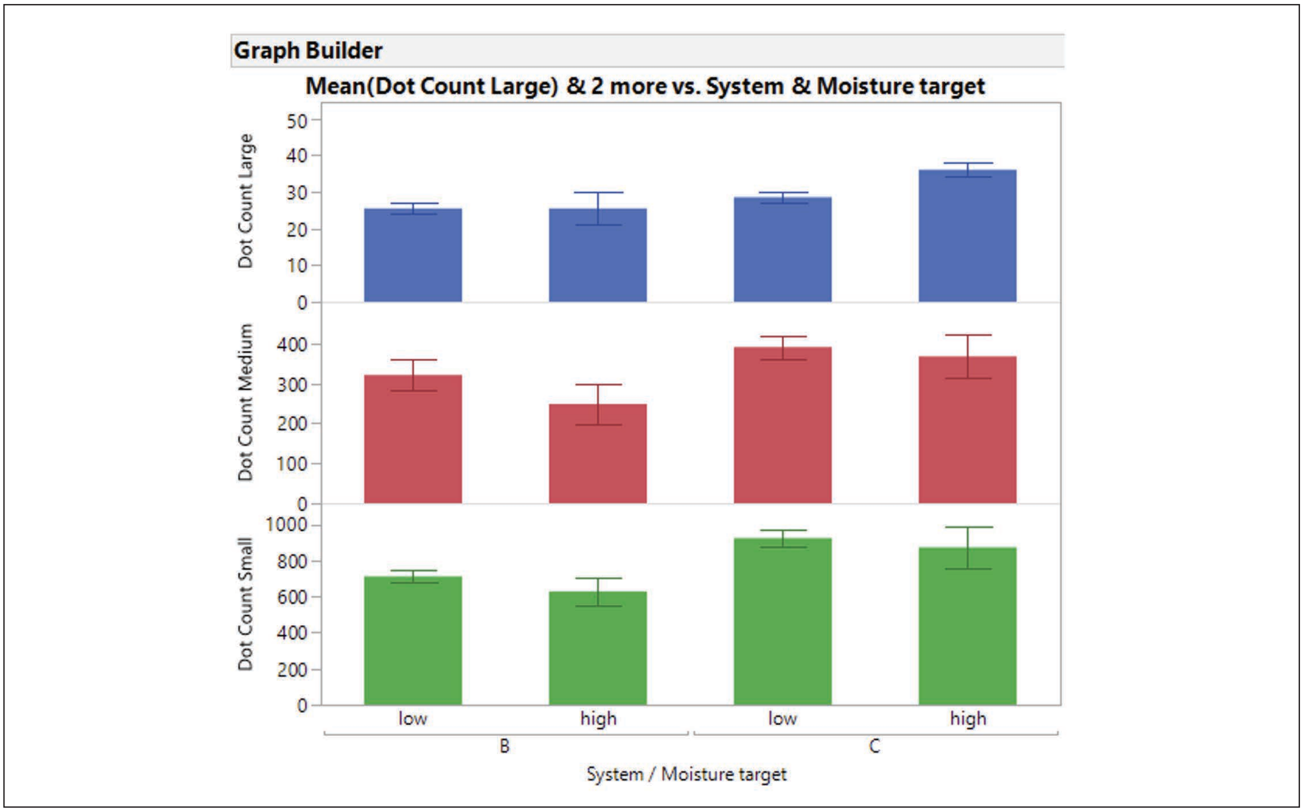

14. Effect of moisture target and coalescing aid (B = no, C = yes).

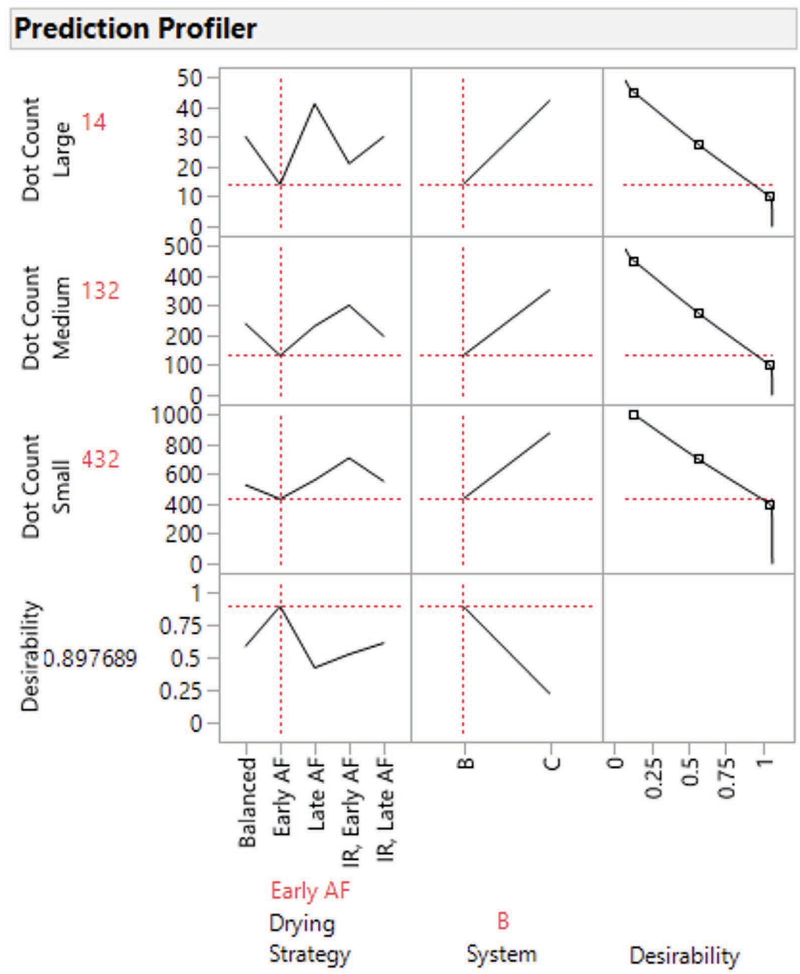

15. Predictive model and drying/chemistry optimization for reduced defects in Study II. See Table IV for descriptions of drying strategies.

lationship between target moisture (when IR drying is used) and the effect of coalescing aid. In all cases, the coalescing aid modification, Barrier System C, resulted in higher dot counts for all three classifications, as presented earlier. It was also observed that the more typical high moisture target (4.3%) led to the fewest defects for the medium and small classifications. This could indicate that the higher drying energy, which produced higher sheet temperatures to drive moisture to the lower target, creates more medium and small defects.

For pilot coater Study II, data could be modeled against the two primary variables of the system (coalescing aid: Barrier System "B" = no; Barrier System "C" = yes"), and **Fig. 15** shows drying strategy at equal final target moisture. In this case, by using a prediction profiling tool, we can determine the optimal set of conditions to minimize the defects (dot count). In this case, not using early IR drying and front-loading the air flotation drying to the earlier dryer sections reduces dot count. As shown earlier, the use of glycerol as a coalescing aid was not effective.

Study III – Barrier system comparison

For this evaluation, a simple dot plot with a smoothed line fit was constructed comparing, for each dot size (large, medium, small), the dot count vs. applied coat weight for the three trial conditions in Study III. The focus of this study is not specifically the chemistry changes, but whether or not the new test method is capable of detecting differences in barrier coating systems. As observed from **Fig. 16**, it is apparent that moving from Barrier System X to Barrier System Y to Barrier System Z shows a marked improvement in reducing the number of defects in all defect classifications. To be stated in another way, for constant coat weight at values below 8 g/m^2, the "Y" and "Z" systems offer more efficient coverage and fewer defects.

For pilot coater Study III, data could be modeled against the two primary variables of the Barrier System ("X" vs. "Y" vs. "Z") and coat weight (**Fig. 17**). With the prediction profiling tool, using statistically significant models for each output, we can determine the optimal system at constant coat weight (minimize the defects/dot count). In this case,

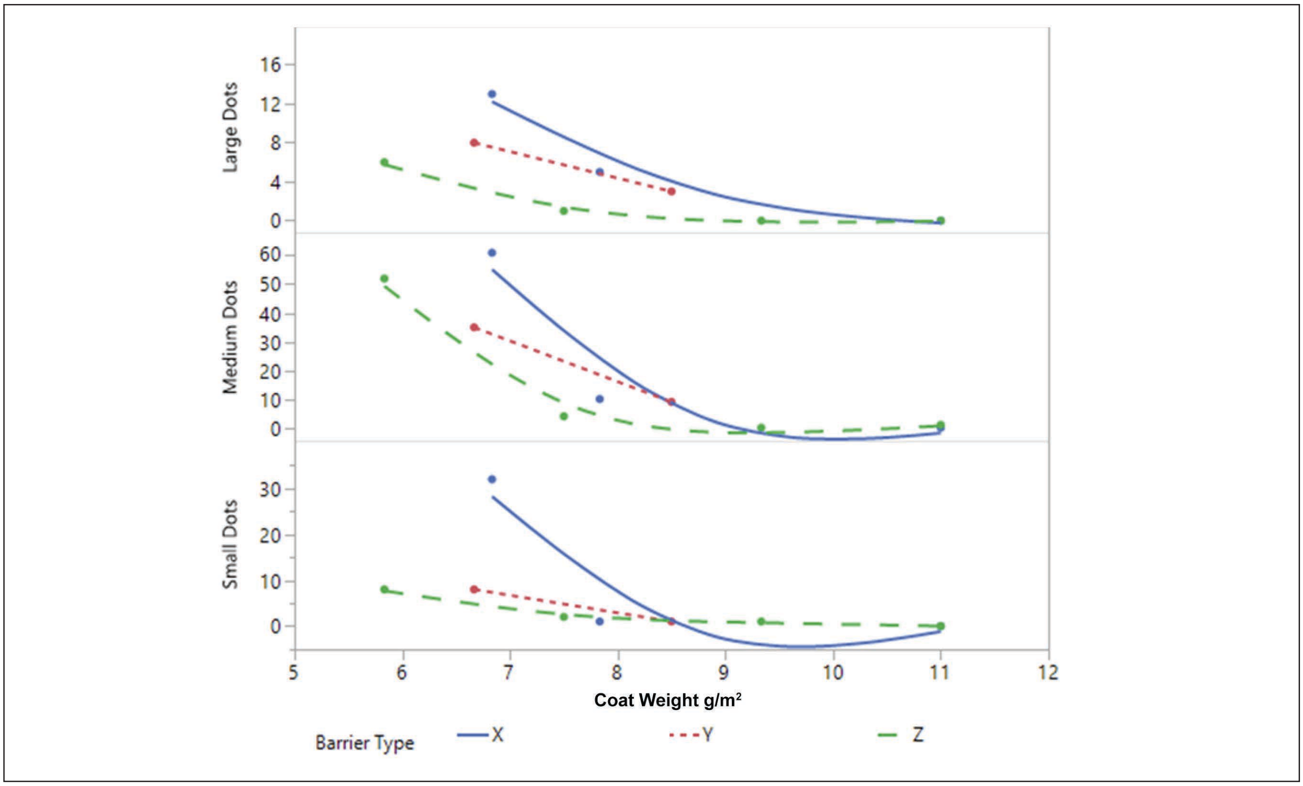

16. Dot size and dot count vs. barrier system type.

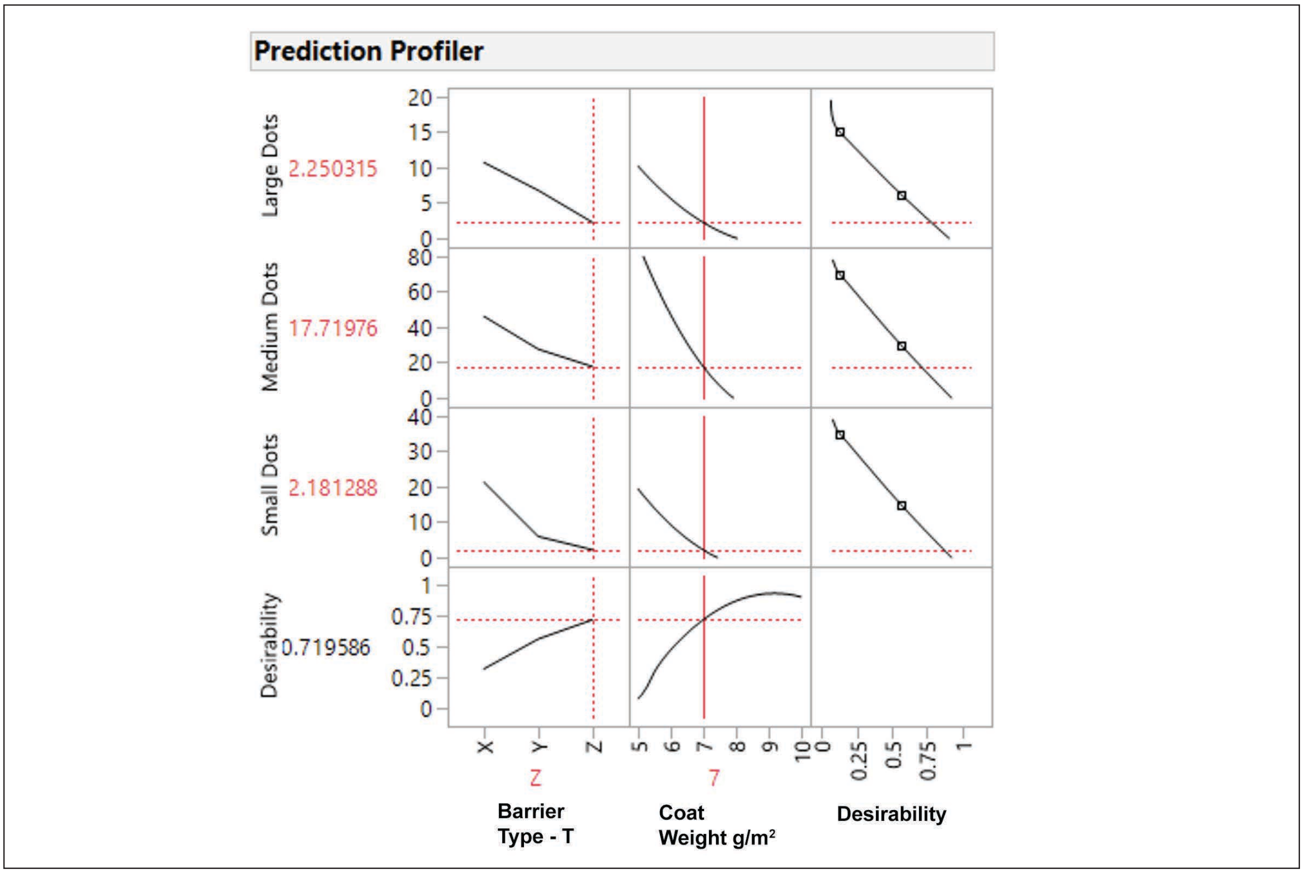

17. Predictive model for barrier type optimization for reduced defects in Study III.

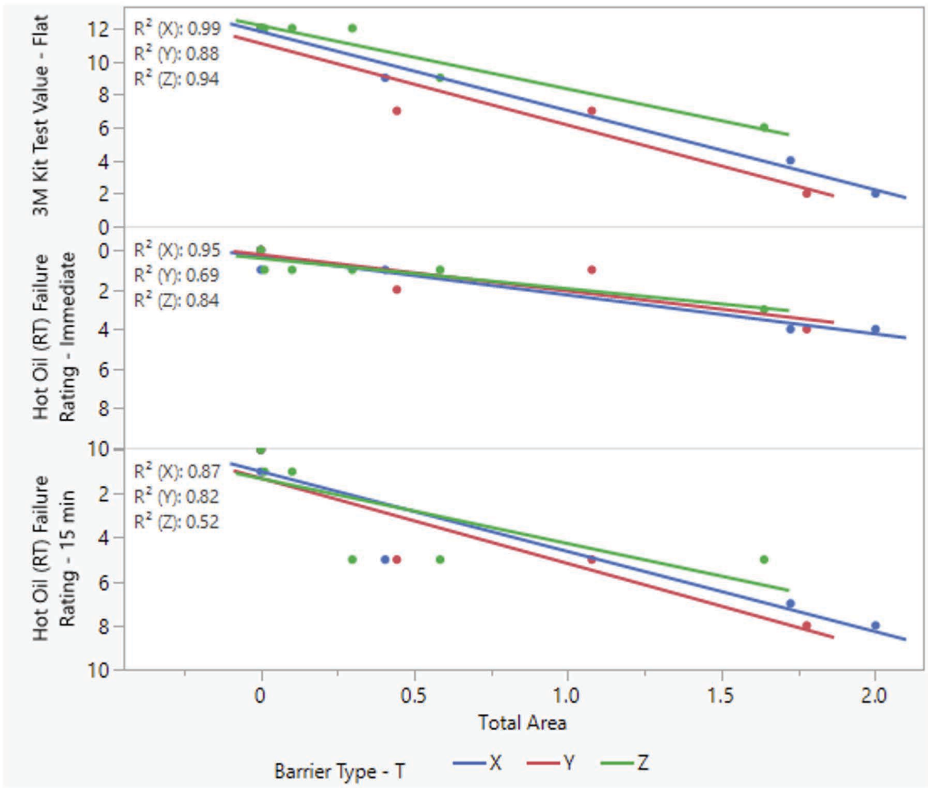

18. Barrier system performance vs. total defect area (R^2 = coefficient of determination).

the data suggest Barrier System Z is the best at 7 g/m² coat weight and lower.

Data from the Defect Characterization test was evaluated for correlation against the two barrier test protocols as presented earlier. For all systems, lower measured defect area correlated well with both barrier test methods, as shown in **Fig. 18**. For each barrier system, a linear fit was performed, and the coefficient of determination (R^2) values are shown. In most cases, the correlation was very good, but it was especially so for the 3M Kit test and the immediate ratings for the Hot Oil test. For the longer time evaluation of the Hot Oil test at 15 min, the R^2 values were not as good, and it appears there could be a step-change in performance that relates to a saturation level reached at total defect area levels above 0.25 mm².

CONCLUSIONS

In conclusion, the Defect Characterization test has been shown to correlate with other barrier test results and has been able to detect defect changes brought about by process and formulation changes. The impact of changes in drying strategy and formulation components were detected and quantitatively measured by the change in size and frequency of film defects. The Defect Characterization test may have a higher upfront cost than the traditional 3M Kit test (if wanting more than pass/fail data), but the accuracy, safety, and ease of conducting the test likely supersede the costs. Although the equipment used for image analysis is extremely helpful to examine the defects in high detail, we do believe a simple application of dyed oil to the substrate can quickly identify basic defects without the use of additional equipment. If only needing pass/fail data, dyed oil is a much cheaper investment than what is required to carry out other barrier testing (various oils, chemicals, fume hoods, ovens, etc.), and there is a substantial cost savings involved. If necessary, the dyed oil can be applied directly to a roll of paper, eliminating the need to slab down rolls to obtain sheet samples, creating significant time savings.

Like the 3M Kit test, other barrier tests require a defect-free surface. Tests such as the Hot Oil Application test, Contact Angle, and even Cobb may give less than desired outcomes if defects are present (premature failures, lower contact angles, complete saturation failures). The Defect Characterization test may not replace these barrier tests but will ensure that additional testing on the substrate will be more accurate. If such coatings have been proven to be effective in the past from a coating design and performance perspective, testing beyond the Defect Characterization test may not even be necessary. **TJ**

ACKNOWLEDGEMENTS

We would like to acknowledge Trinseo LLC for sponsoring this research paper. Additionally, the efforts of the staff members at the pilot coater and testing labs in Midland, MI, USA, are greatly appreciated. We also wish to thank Dr. Pekka Salminen for his support in providing the references relating to fluid transport theory for barrier coating performance.

LITERATURE CITED

1. Smithers Pira, "The future of functional and barrier coatings for paper and board to 2024," Smithers Pira, Leatherhead, Surrey, UK, 2019.
2. Luyken, H., "Water height in a capillary tube plotted against diameter," personal work, Wikipedia. Available [Online] https://en.wikipedia.org/wiki/Jurins_law <18Nov2021>.
3. Konečný, E., "Illustration of capillary rise," personal work, Wikipedia. Available [Online] https://en.wikipedia.org/wiki/Young%E2%80%93Laplace_equation <18Nov2021>.
4. Sahasrabudhe, S.N., Rodriguez-Martinez, V., O'Meara, M., et al., *Int. J. Food Prop.* 20(sup 2): 1965(2017). https://doi.org/10.1080/10942912.2017.1360905.
5. Emilsson, P., "Multi layers to drying strategy to avoid pinholes by sustainable barrier coating," *PaperCon*, TAPPI Press, Peachtree Corners, GA, USA, 2017.
6. Habermahl, L.K., Pollock, M., Attal, J., et al., *TAPPI Coat. Conf.*, TAPPI Press, Atlanta, 1997, p. 111.
7. Yang, A., Salminen, P., Vervoort, S., et al., *Appl. Rheol.* 21(2): 23607(2011). https://doi.org/10.3933/applrheol-21-23607.

ABOUT THIS PAPER

Cite this article as:
Burton, D., Ventresca, D., and Welsch, G.W., *TAPPI J.* 21(11):625(2022). https://doi.org/10.32964/TJ21.11.625

DOI: https://doi.org/10.32964/TJ21.11.625

ISSN: 0734-1415

Publisher: TAPPI Press

About this journal

ABOUT THE AUTHORS

Burton

Ventresca

Welsch

As the local barrier capabilities expert within Trinseo, I (Burton) spend much of my day working with, testing, and developing barrier coatings. I have noticed that the existing tests associated with barrier coatings are lackluster and need improvements. This research compliments existing barrier-type testing, improving its accuracy by determining whether the face of the sheet is defect free before performing any other forms of barrier-type testing.

The most difficult aspect of this study was determining how to analyze the data. I discovered that if we used a dyed oil rather than a natural-occurring color, the defects become more apparent and the color can then be extracted using existing analytical extraction methods to give accurate counts of dyed defects.

An interesting finding in this work has been how many customers have been waiting for a test like the Defect Characterization test presented here, and how many really dislike existing test methods. It was also surprising to find that a number of commercially available products have defects on the surface.

For mills, the Defect Characterization test can be completed in a short amount of time using a small paper sample. The next step in this work is to determine what the shape of defects is trying to tell us. Can we pinpoint if the defect is a fisheye, undercoated fiber, pinhole, or blister? There is also more work to be done in determining whether the type of defect affects the overall performance of the barrier.

Burton is senior research technologist and Welsch is Global Innovation leader for Trinseo LLC in Midland, MI, USA. Ventresca is technical service and development specialist for Trinseo LLC in Petrolia, ON, Canada. Email Burton at DBurton@trinseo.com.

APPENDIX

Reference equations

Young-Laplace equation

Simplified equation for a capillary tube:

$$\Delta p = \frac{2\gamma}{R}.$$

where:

Δp = differential pressure between the two ends

γ = surface tension

R = radius of the capillary

Hagen-Poiseuill equation

$$\Delta p = \frac{8\mu LQ}{\pi R^4} = \frac{8\pi\mu LQ}{A^2} \quad \text{or} \quad Q = \frac{\pi \Delta p r^4}{8 \mu L}$$

where:

Δp = differential pressure between the two ends

L = length of the pipe

μ = dynamic viscosity

γ = surface tension

Q = volumetric flow rate

R = pipe radius

A = cross-section of the pipe

Study I data

Study I data was derived from analyzing data from Study III with modeling and data analysis on base sheet changes, as shown in the following table.

RUN NUMBER	11.0	11.1	11.2	12.0	12.1	12.2	19.0	19.1	20.0	20.1	17.0	17.1	17.2	17.3	18.0	18.1	18.2
BASESHEET	H	H	H	I	I	I	H	H	I	I	H	H	H	H	I	I	I
MACHINE SETTINGS																	
Blade (B=Bent)	20-45	20-45	20-45	20-45	20-45	20-45	20-45	20-45	20-45	20-45	20-45	20-45	20-45	20-45	20-45	20-45	20-45
Rod (G=Grooved)																	
Head Angle	49.7	49.7	49.7	49.7	49.7	49.7	49.7	49.7	49.7	49.7	49.7	49.7	49.7	49.7	49.7	49.7	49.7
Head Stops (in.)																	
Applicator Roll Speed (%)	22	22	22	22	22	22	22	22	22	22	22	22	22	22	22	22	22
Applicator Roll Gap (in.)																	
Coater Speed (FPM)	1500	1500	1500	1500	1500	1500	1500	1500	1500	1500	1500	1500	1500	1500	1500	1500	1500
Coated Side	Felt	Felt	Felt	Inside	Inside	Inside	Felt	Felt	Inside	Inside	Felt	Felt	Felt	Felt	Inside	Inside	Inside
RUN VARIABLES																	
Basestock Moisture (%)	3.8	3.8	3.7	3.4	3.2	3.2	3.6	3.6	3.2	3.3	3.9	3.8	3.6	3.5	3.5	3.4	3.2
Coat Weight (lbs./3300 SF)	4.1	4.7	6.6	3.8	4.8	7	4	5.1	3.6	5.7	4.5	5.6	6.6	3.5	4.2	6.2	7.6
Moisture (%)	3.6	4.1	4.1	4.1	4.4	4.3	4	4	4.5	5.6	4.2	4.6	4.5	3.5	4.2	3.8	4.1
Tube Load (PSI)	23.9	13.9	6	16.1	9.5	5	19.4	11.9	15.9	6	23.9	21	12.9	23.8	16.9	10.9	8

Study II data

Formulation	B	C
Parts		
Modified proprietary SA-SCE barrier system	100	100
Coalescing aid	0	1
Associative thickener	0.5	0.5
Defoamer	0.07	0.07
Testing		
% Solids	44.6	44.3
pH NaOH	8.0	8.0
Viscosity @ 20 rpm, w/#4	3550	3180
Viscosity @ 100 rpm, w/#4	1268	1176
Hercules max rpm viscosity	54.9	48.3

NaOH = sodium hydroxide.

RUN NUMBER		3	4	5	6	7	8	9	10	11	12	13	14	15	16
FORMULATION		B	B	B	B	B	C	C	C	C	C	B	B	C	C
MACHINE SETTINGS															
Blade	(B=Bent)	15/40	15/40	15/40	15/40	15/40	15/40	15/40	15/40	15/40	15/40	15/40	15/40	15/40	15/40
Rod	(G=Grooved)														
Head Angle		44.7	44.7	44.7	44.7	44.7	44.7	44.7	44.7	44.7	44.7	44.7	44.7	44.7	44.7
Applicator Roll Speed	(%)	22	22	22	22	22	22	22	22	22	22	22	22	22	22
Coater Speed	(FPM)	1500	1500	1500	1500	1500	1500	1500	1500	1500	1500	1500	1500	1500	1500
RUN VARIABLES															
Basestock Moisture	(%)	6.8	6.5	6.1	6.3	6.0	7.1	7.0	6.8	6.9	6.8	6.4	6.0	7.0	6.7
Coat Weight	(lbs./3300 SF)	3.7	3.9	3.9	3.9	3.9	3.8	4.0	4.0	3.9	4.0	4.1	4.0	4.3	4.1
Moisture	(%)	4.4	4.4	4.1	4.3	4.2	3.6	4.6	4.4	4.3	4.4	2.2	2.8	2.9	2.7
Tube Load	(PSI)	9.8	8.0	7.6	7.9	7.1	8.9	6.3	6.2	5.9	6.2	7.7	7.3	6.0	6.3
DRYER SETTINGS															
IR Preheat	(%)	100	100	100	100	100	100	100	100	100	100	100	100	100	100
IR Zone 1	(%)	100	100	100			100	100	100			100	100	100	100
IR Zone 2	(%)		100	100				100	100			100	100	100	100
TEC 1 Temperature	(°F)	250		400		475	300		400		500		500		500
Pressure	(in. of water)	0.7		1		1.3	1.3		1		1.5		1.5		1.5
TEC 2 Temperature	(°F)	250		400		475	300		400		500		500		500
Pressure	(in. of water)	0.7		1		1.3	1.3		1		1.5		1.5		1.5
TEC 3 Temperature	(°F)	250	250		375		300	250		400		400		400	
Pressure	(in. of water)	0.7	1		1		1.3	1.7		1.3		1		1.3	
TEC 4 Temperature	(°F)	250	250		375		300	250		400		400		400	
Pressure	(in. of water)	0.7	1		1		1.3	1.7		1.3		1		1.3	
SHEET TEMPERATURE															
IR Preheat	(°F)	144	146	149	147	149	145	145	147	146	148	147	149	145	147
Before TEC 1	(°F)	117	153	155	87	90	114	152	153	87	87	154	155	152	154
After TEC 1	(°F)	119	107	140	92	140	116	97	125	85	132	104	165	95	152
After TEC 2	(°F)	130	111	156	92	175	137	103	152	87	184	106	190	99	192
After TEC 3	(°F)	145	144	140	146	134	154	144	138	147	132	165	150	160	149
After TEC 4	(°F)	158	160	146	173	134	173	159	140	177	125	200	149	189	142
Reel	(°F)	86	86	86	86	86	86	86	86	89	87	89	87	89	88

Study III data

Formulation	X	Y	Z
Parts			
Proprietary SA-SCE Barrier System X	100	100	
Proprietary SA-SCE Barrier System Z			100
Na DOSS		0.5	
Alcogum L229	0.5	0.5	0.5
Foamaster	0.05	0.05	0.05
Test Results			
% Solids	47.1	47.1	47.5
pH NaOH	7.9	7.9	7.8
Viscosity @ 100 rpm, w/#	1460	1870	2212
Hercules maximum rpm viscosity	72.0	89.1	89.4

Na DOSS = sodium dioctyl sulfosuccinate wetting agent; Alcogum L229 = rheology modifier and wetting agent from Nouryon (Amsterdam); Foamaster = mineral oil defoamer from BASF (Ludwigshafen; Germany); NaOH = sodium hydroxide.

RUN NUMBER	11.0	11.1	11.2	12.0	12.1	12.2	19.0	19.1	20.0	20.1	17.0	17.1	17.2	17.3	18.0	18.1	18.2
FORMULATION	**X**	**X**	**X**	**X**	**X**	**X**	**Y**	**Y**	**Y**	**Y**	**Z**	**Z**	**Z**	**Z**	**Z**	**Z**	**Z**
MACHINE SETTINGS																	
Blade (B=Bent)	20-45	20-45	20-45	20-45	20-45	20-45	20-45	20-45	20-45	20-45	20-45	20-45	20-45	20-45	20-45	20-45	20-45
Rod (G=Grooved)																	
Head Angle	49.7	49.7	49.7	49.7	49.7	49.7	49.7	49.7	49.7	49.7	49.7	49.7	49.7	49.7	49.7	49.7	49.7
Head Stops (in.)																	
Applicator Roll Speed (%)	22	22	22	22	22	22	22	22	22	22	22	22	22	22	22	22	22
Applicator Roll Gap (in.)																	
Coater Speed (FPM)	1500	1500	1500	1500	1500	1500	1500	1500	1500	1500	1500	1500	1500	1500	1500	1500	1500
Coated Side	Felt	Felt	Felt	Inside	Inside	Inside	Felt	Felt	Inside	Inside	Felt	Felt	Felt	Felt	Inside	Inside	Inside
RUN VARIABLES																	
Basestock Moisture (%)	3.8	3.8	3.7	3.4	3.2	3.2	3.6	3.6	3.2	3.3	3.9	3.8	3.6	3.5	3.5	3.4	3.2
Coat Weight (lbs./3300 SF)	4.1	4.7	6.6	3.8	4.8	7	4	5.1	3.6	5.7	4.5	5.6	6.6	3.5	4.2	6.2	7.6
Moisture (%)	3.6	4.1	4.1	4.1	4.4	4.3	4	4	4.5	5.6	4.2	4.6	4.5	3.5	4.2	3.8	4.1
Tube Load (PSI)	23.9	13.9	6	16.1	9.5	5	19.4	11.9	15.9	6	23.9	21	12.9	23.8	16.9	10.9	8
DRYER SETTINGS																	
IR Preheat (%)																	
IR Zone 1 (%)																	
IR Zone 2 (%)																	
TEC 1 Temperature (°F)	275	275	450	350	350	475	300	375	325	350	325	375	500	350	375	500	500
Pressure (in. of water)	0.5	0.5	1	1.5	1.5	1.5	1	1.5	1	2	0.7	1	1.3	0.5	1	1.5	1.5
TEC 2 Temperature (°F)	275	275	450	350	350	475	300	375	325	350	325	375	500	350	375	500	500
Pressure (in. of water)	0.5	0.5	1	1.5	1.5	1.5	1	1.5	1	2	0.7	1	1.3	0.5	1	1.5	1.5
TEC 3 Temperature (°F)	275	275	450	350	350	475	300	375	325	350	325	375	500	350	375	500	500
Pressure (in. of water)	0.5	0.5	1	1.5	1.5	1.5	1	1.5	1	2	0.7	1	1.3	0.5	1	1.5	1.5
TEC 4 Temperature (°F)	175	175	450	350	350	475	300	375	325	250	325	175	175	350	175	300	175
Pressure (in. of water)	0.5	0.5	1	1.5	1.5	1.5	1	1.5	1	2	0.7	1	1.3	0.5	1	1.3	1.3
SHEET TEMPERATURE																	
IR Preheat (°F)	72	72	72	74	73	73	69	69	70	70	73	72	68	69	69	69	69
Before TEC 1 (°F)	74	74	72	74	74	74	71	71	71	71	76	76	70	70	69	69	70
After TEC 1 (°F)	119	116	132	126	128	137	116	124	122	126	122	130	136	121	128	139	144
After TEC 2 (°F)	128	124	138	158	144	150	134	146	147	140	128	135	155	146	155	170	177
After TEC 3 (°F)	149	138	170	189	184	199	157	177	178	183	149	167	194	164	193	217	231
After TEC 4 (°F)	139	140	189	206	207	224	178	199	199	194	170	170	168	174	213	218	206
Reel (°F)	79	79	85	98	105	110	82	84	96	101	89	92	84	82	96	103	104